Application Note

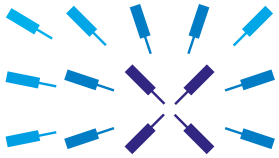

Zurich Instruments

Active Reset of Superconducting Qubits

Applications: Quantum Computing, Circuit QED
Products: UHFLI, UHF-AWG, UHF-DIG

Release date: July 2017

Introduction

A quantum computer is potentially able to tackle computational problems that a classical computer can't solve in practice [1, 2]. Among the criteria that such a device must fulfill [3] is the capability to initialize the state of its basic building blocks, the qubits, with high fidelity. Here we demonstrate a 10-fold speed-up in reset for a given fidelity and a 10-fold improvement for the final state preparation fidelity using an active reset method for superconducting qubits.

The method consists of a single-shot measurement of the qubit's state followed by a conditional single-qubit gate operation that rotates the qubit into the ground state, in case it was found in the excited state [4]. We compare the method with the simpler alternative for state initialization, passive waiting for qubit decay, and quantify the speed and fidelity advantage of the active method. Speed is relevant for achieving high experimental repetition rates. The speed of the active method is mostly limited by the achievable feedback latency. The speed of the passive method is limited by the qubit lifetime making it impractical in view of the advances in fabrication leading to ever improving qubit lifetimes. The fidelity of the active method can exceed the limit set by the system temperature which applies to the passive method.

The main challenge in implementing active qubit reset is the requirement for low-latency signal processing and conditional signal generation. The Zurich Instruments UHFLI enables feedback on the scale of a microsecond thanks to it incorporating a fast digital lock-in amplifier, an arbitrary waveform generator, and a cross-domain trigger engine linking the two. The UHFLI thus makes active qubit reset available without the cost of developing and maintaining a customized digital signal processing solution [4].

Setup and Sample

The sample we used is shown in Figure 1 (a) and consists of niobium- and aluminium-based resonant circuits on a sapphire substrate. For a detailed description of the sample see Ref. [5]. The qubit shown in the inset is a nonlinear resonator formed of a small superconducting quantum interference device (SQUID) acting as a non-linear inductor and an on-chip capacitor (orange in the image). The SQUID design makes the qubit frequency tunable over a frequency range from 4 to 7.5 GHz by applying a small magnetic field to the device. A coplanar waveguide (green) directs external control signals to the qubit. The qubit is coupled to a coplanar-waveguide resonator (blue) [6] with a frequency of 4.78 GHz. This readout resonator is connected through an on-chip Purcell filter to a pair of coaxial cables that provide the interface for reading out the quantum state of the qubit. Figure 1 (b) depicts a schematic of the measurement setup in which the sample is installed in a dilution refrigerator to provide a well isolated low-temperature environment protecting the quantum properties of the sample.

The control pulses are generated by quadrature modulation of a microwave signal using two AWG channels. The pulses for qubit readout are generated by feeding one of the AWG marker channels to the gate input of a microwave frequency signal generator. After transmission through the readout resonator, the pulses are amplified using a parametric amplifier followed by low-noise cryogenic and room-temperature amplifiers. The signal is then down-converted in the analog domain to an intermediate frequency f_{IF} of 28.125 MHz. Using one of the UHFLI lock-in amplifier channels, the signal is further down-converted in the digital domain. The resulting in-phase and quadrature component signals are then digitized using the UHF-DIG Digitizer

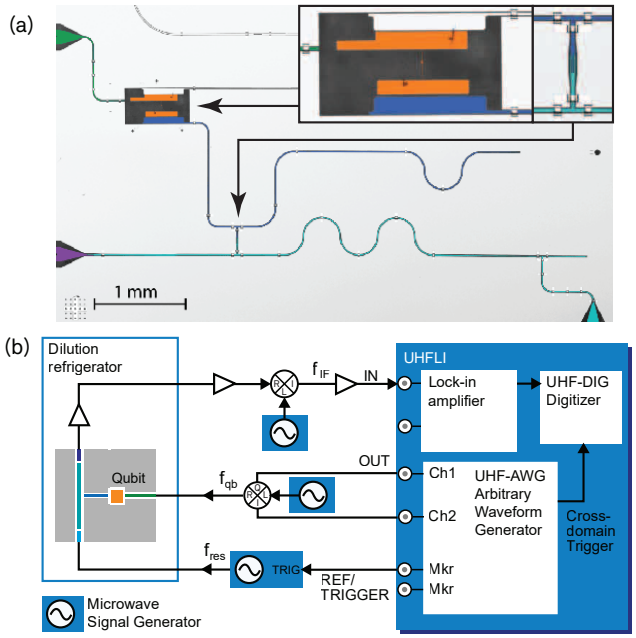

Figure 1. (a) Optical micrograph of the sample showing the readout resonator (blue) and the qubit capacitor plates (orange). The resonator is coupled to input and output lines via a Purcell filter [7] (cyan). Insets show magnified views of the qubit and the coupler between resonator and Purcell filter. (b) Simplified diagram of the experimental setup based on the UHFLI instrument integrating a lock-in amplifier and an AWG. The superconducting qubit sample is cooled in a dilution refrigerator.

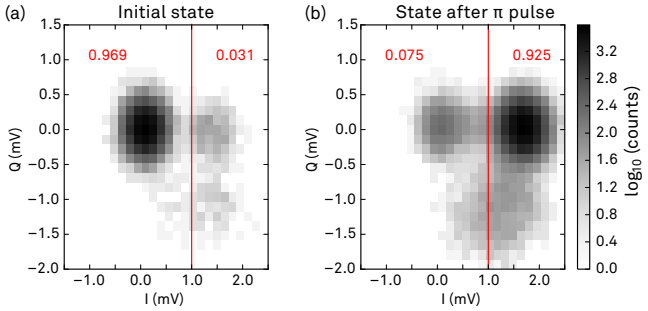

Figure 2. Histograms of integrated signal quadratures in repeated single-shot state measurement. (a) shows the histogram when measuring the qubit in its thermal equilibrium ground state after waiting a time much longer than the qubit lifetime before taking an individual measurement. (b) shows the histogram of measurements taken after having applied a π pulse to the qubit. The two maxima in the histogram in (a) and (b) are identified with the qubit's ground and excited state, respectively. The red numbers are the relative fraction of counts in the areas delimited by red lines which represent the state discrimination threshold used for active qubit reset. The population of the ground state in (b) is mainly caused by relaxation during the readout.

module of the UHF instrument.
Qubit Rabi oscillation measurements were carried out as described in Ref. [8]. Using such measurements we identified the optimum set of parameters of the qubit π control pulse used to excite and reset the qubit. We used a first-order DRAG pulse shape as described in Ref. [9].

Active qubit reset

Single-shot qubit measurement

The measurement of the initial qubit state marks the start of the active qubit reset cycle. The qubit state is determined by measuring the downconverted pulsed readout signal with the lock-in amplifier and comparing the acquired quadrature voltage most sensitive to the qubit state change to a threshold value. The high-performance amplification chain based on the parametric amplifier allows us to reach a signal-to-noise ratio sufficiently large to discriminate the qubit states in a single shot without averaging over repeated experiments. The ability to perform single-shot readout is a prerequisite for active qubit reset.
Figure 2 shows the histogram of the measured signal quadratures over 40,000 repetitions of the same experiment. For the measurement in Figure 2 (a), no control pulse was applied prior to the state measurement, and the qubit is thus expected to be in thermal equilibrium close to the ground state (passive reset). In Figure 2 (b), a π pulse was applied immediately before the state measurement. There we identify two local maxima corresponding to the qubit ground and first excited states, and a weaker maximum in the bottom half of the plot presumably due to population of the second excited state. The predominant part of the contrast for the state measurement is contained in the in-phase (I) signal component. We set the threshold for state discrimination to 1 mV (red vertical lines).

Implementing feedback with the UHF-AWG

We configure the internal cross-domain trigger of the UHFLI to perform the qubit state discrimination. The digital signal following this discrimination is used to define a sequence branching point in the UHF-AWG sequence program which determines whether the AWG will output a dual-channel π pulse, or no signal.
The LabOne AWG Sequencer allows one to formulate the corresponding hardware instructions in an easily readable, high-level programming language called SeqC. The core part of that program is shown in Figure 3. The first instruction in the program initiates the playback of the waveform `w_read`. This waveform contains a digital marker that is used as a gate signal to generate a readout microwave pulse. Following the playback, the sequencer is instructed to wait during `wait_time` until the cross-domain trigger engine has executed the state discrimination operation and the readout signal is available. The binary result of the discrimination is then read by the sequencer and stored in the run-time variable `qb_state`.
The subsequent switch statement contains two branches, one of which is executed conditioned on the value of `qb_state` (0 or 1). One branch corresponds to the dual-channel playback of the waveforms `w_pi_1` and `w_pi_2` (the qubit π pulse), the other branch is the playback of the zero-valued waveforms `w_zero_1` and `w_zero_2` of the same length. The waveforms used in this part of the program are defined in the same

```
// Apply readout pulse:
playWave(w_read);

// Wait until the readout result is available
wait(wait_time);

// Read the digital state of the trigger
    configured with the I quadrature as input and
    a discrimination threshold of 1 mV
qb_state = getAnaTrigger(1);

// Apply pi pulse if the qubit was in the excited
    state
switch (qb_state) {
  case 0:
    playWave(w_pi_1, w_pi_2);
  case 1:
    playWave(w_zero_1, w_zero_2);
  default:
}
```

Figure 3. Core part of the sequence program in the SeqC language used to control the conditional feedback action.

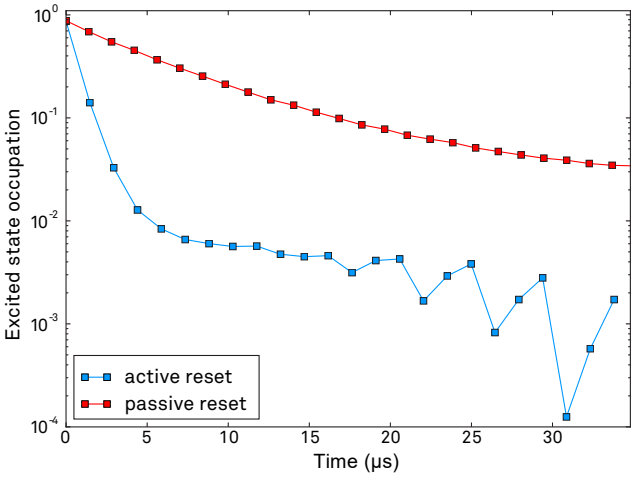

Figure 4. Time evolution of the averaged qubit excited-state occupation with active and passive qubit reset, respectively. Before the start of the protocol, the qubit is initialized by applying a π pulse. Every 1.48 microseconds, a state measurement is taken. After each measurement, a conditional π pulse is applied to initiate an active reset, or no pulse is applied for passive reset.

program (not shown) using mathematical functions that are evaluated by the compiler.

Repeated active qubit reset

The effectiveness of the qubit reset can be improved by repeating the feedback cycle described above. This allows us to reach a sub-percent-level excited-state population, much better than what would be possible by using a single feedback cycle. Repetition of the cycle is easily achieved by looping over the code segment shown above.

The blue curve in Figure 4 shows the evolution of the qubit state during a qubit reset protocol consisting of 23 repetitions of a feedback cycle. The blue squares represent the excited-state population averaged over 40,000 repetitions of the experiment. In order to compare the decay curve with the one observed without active reset, a control experiment was done where the qubit state was read out repeatedly in the same way as with active reset enabled, but without a π pulse applied to the qubit. The decay curve without feedback, but with repeated measurements, is identical to a decay curve measured with a conventional T_1 measurement such as the one described in [8].

After the first feedback cycle or 1.48 µs, the qubit excited state population has dropped to about 12 %. Using the passive method, reaching this level takes about 14 µs. After 4 to 5 repetitions, the initially fast decay gradually becomes slower but the excited-state population continues to decrease. After 23 feedback repetitions, it has dropped to below 0.3 %, whereas in the passive method the residual occupation converges to 3 % after a long waiting time, also cf. the measurement in Figure 2 (a).

Feedback latency

Feedback latency is a key specification determining the fidelity of the active qubit reset. A small latency reduces the main source of error occurring during each feedback cycle, spontaneous qubit decay occurring between the readout and the π pulse. In the present example, this mechanism accounts for about 19 % error calculated from the qubit's lifetime T_1 of 7.1 µs and the period 1.48 µs of one complete feedback cycle. In addition, a small latency implies that more reset cycles can be completed in the same amount of time. In the following, we present measurements of the feedback latency in the configuration used for the experiment discussed above.

Figure 5 depicts the setup used for these measurements. In comparison to the setup in Figure 1, the wiring is changed such that the qubit control signals as well as the readout return signal are rerouted to an oscilloscope. The UHFLI therefore doesn't receive a readout signal, and the control signals generated by the UHF-AWG do not reach the qubit. However, as the signal processing latency in the UHFLI instrument is unaffected by these changes, the setup allows us to observe the same latency that would apply to the actual measurement, referenced to the plane of the UHFLI Signal Input and Output connectors.

Figure 6 shows the qubit readout and control signals measured in this configurations. The readout signal (top) at the intermediate frequency has been averaged over multiple scope acquisitions in order to make its timing clearly visible despite the noise. From the beginning of the readout signal burst to the beginning of the qubit control pulses generated by the AWG, we measure a latency of 1.12 µs. Part of this time is the signal integration time of 0.37 µs that allowed us to reach a sufficiently high SNR for the single-shot readout. The remaining part, about 0.75 µs, comes from

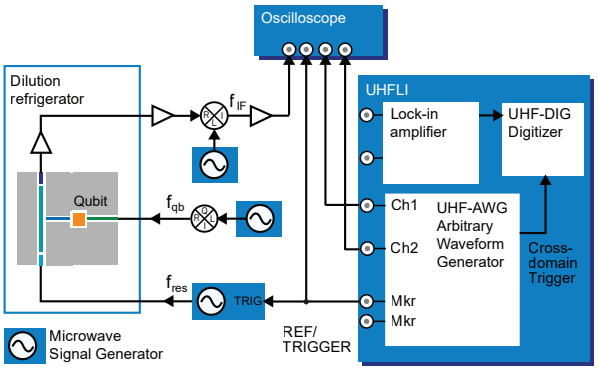

Figure 5. Setup used to measure the feedback latency of the active qubit reset. The qubit control signals and the qubit readout signals are routed with cables of equal length from the UHFLI to an oscilloscope. The gate signal generated by the UHF-AWG marker channel 1 is connected to the oscilloscope via a T-piece for triggering. The UHF-AWG Sequencer executes the same program as in the experiment, which makes the timing in this measurement equal to the timing in the actual experiment.

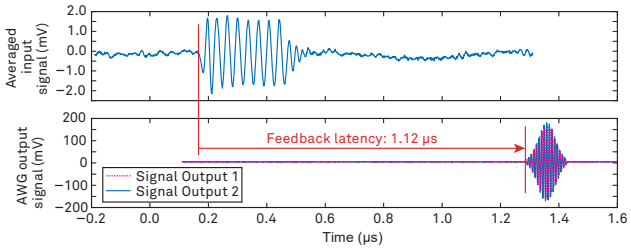

Figure 6. Measurement of the feedback latency of the UHF instrument referenced to its front panel connectors. The dual-channel AWG signal starts 1.12 µs after the start of the readout pulse. The input signal has been averaged in order to identify the start of the readout pulse using an oscilloscope.

other signal processing such as A/D and D/A conversion or demodulation and represents the minimum latency that can be achieved with the UHF instrument.

Conclusion

The measurements shown above quantify the benefits of the active qubit reset method and demonstrate the ease of its implementation with the UHFLI Lock-in Amplifier and the UHF-AWG Arbitrary Waveform Generator. In a concrete example, we achieved a ten-fold speed-up in reset for a given fidelity and a ten-fold improvement for the final state preparation fidelity compared to the passive reset method. These results build on powerful, low-latency digital signal processing tools available on the Zurich Instruments UHF instrument. Flexible extension to multi-qubit measurement and control systems is enabled by the possibility to perform demodulation at multiple frequencies with the UHF-MF option. Multiple AWG sequence branches also enable more complex feedback protocols, e.g. taking into account detection of higher excited states.

Acknowledgements

Zurich Instruments would like to thank Prof. Wallraff and the members of his Quantum Device Lab at ETH Zurich, Switzerland, in which these measurements were carried out. Special thanks go to Michele Collodo. We thank Theodore Walter for providing the qubit sample and Yves Salathé, Simone Gasparinetti, and Philipp Kurpiers for support with the measurements and for discussions.
This work was supported by the Swiss Federal Department of Economic Affairs, Education and Research through the Commision for Technology and Innovation (CTI).

References

[1] R. P. Feynman. Simulating physics with computers. Int. J. of Theor. Phys., 21:467, 1982.

[2] T. D. Ladd, F. Jelezko, R. Laflamme, Y. Nakamura, C. Monroe, and J. L. O'Brien. Quantum computers. Nature, 464:45, 2010.

[3] David P. DiVincenzo. The physical implementation of quantum computation. arXiv:quant-ph/0002077, 2000.

[4] D. Ristè, C. C. Bultink, K. W. Lehnert, and L. DiCarlo. Feedback control of a solid-state qubit using high-fidelity projective measurement. Phys. Rev. Lett., 109:240502, 2012.

[5] T. Walter, P. Kurpiers, S. Gasparinetti, P. Magnard, A. Potocnik, Y. Salathé, M. Pechal, M. Mondal, M. Oppliger, C. Eichler, and A. Wallraff. Rapid high-fidelity single-shot dispersive readout of superconducting qubits. Phys. Rev. Applied, 7:054020, May 2017.

[6] A. Wallraff, D. I. Schuster, A. Blais, L. Frunzio, R.-S. Huang, J. Majer, S. Kumar, S. M. Girvin, and R. J. Schoelkopf. Strong coupling of a single photon to a superconducting qubit using circuit quantum electrodynamics. Nature, 431:1627, 2004.

[7] M. D. Reed, B. R. Johnson, A. A. Houck, L. DiCarlo, J. M. Chow, D. I. Schuster, L. Frunzio, and R. J. Schoelkopf. Fast reset and suppressing spontaneous emission of a superconducting qubit. Applied Physics Letters, 96:203110, 2010.

[8] Zurich Instruments AG. Superconducting Qubit Characterization, 2016. Application Note.

[9] F. Motzoi, J. M. Gambetta, P. Rebentrost, and F. K. Wilhelm. Simple pulses for elimination of leakage in weakly nonlinear qubits. Phys. Rev. Lett., 103:110501, 2009.

Zurich Instruments
Technoparkstrasse 1
CH-8005 Zurich
Switzerland
www.zhinst.com
info@zhinst.com
+41 44 515 04 10